

Out-of-time-ordered commutators in Dirac–Weyl systems

Z. Okvátovity^{1,*} and B. Dóra¹

¹*Department of Theoretical Physics and MTA-BME Lendület Topology and Correlation Research Group,
Budapest University of Technology and Economics, 1521 Budapest, Hungary*

(Dated: September 23, 2019)

Quantum information stored in local operators spreads over other degrees of freedom of the system during time evolution, known as scrambling. This process is conveniently characterized by the out-of-time-order commutators (OTOC), whose time dependence reveals salient aspects of the system’s dynamics. Here we study the spatially local spin correlation function i.e., the expectation value of spin commutator and the corresponding OTOC of Dirac–Weyl systems in 1, 2 and 3 spatial dimensions. The OTOC can be written as the square of the expectation value of the commutator and the variance of the commutator. The problem features only two energy scales, the chemical potential, and the high energy cutoff, therefore the time evolution is separated into three different regions. The spin correlation function grows linearly with time initially and decays in a power-law fashion for intermediate and late times. The OTOC reveals a universal t^2 initial growth from both the commutator and the variance. Its intermediate and late time power-law decays are identical and originate from the variance of the commutator. These results indicate that Dirac–Weyl systems are slow information scramblers and are essential when additional channels for scrambling, i.e. interaction or disorder are analyzed.

I. INTRODUCTION

In recent studies, the chaotic behavior of quantum systems has been investigated from different viewpoints^{1–3}. A common property of chaotic systems is that during unitary time evolution, simple operators can become highly complicated. This leads to the scrambling of information stored in local operator⁴. This phenomena is investigated in different contexts i.e., random matrix theory⁵, black holes³ and quantum thermalisation^{6,7}.

There are multiple ways to characterize chaos and information scrambling e.g. operator entanglement entropy or out-of-time-ordered commutator (OTOC)^{8,9}. In this paper, we are focusing on the latter which was originally introduced by Larkin and Ovchinnikov in 1969 in a calculation of the non-linear correction to the conductivity of a dirty superconductor¹⁰. The OTOC can be considered as the second moment of the commutator, defined as

$$C(t) = -\langle [W(t), V(0)]^2 \rangle \geq 0, \quad (1)$$

where W and V are local operators possibly separated by finite distance and $W(t) = \exp(iHt)W \exp(-iHt)$ denotes the Heisenberg time evolution.

The OTOC is a useful tool to measure the sensitivity of the time evolution of the system on the initial conditions² and to characterize information spreading processes. The information stored in local operators are spreading over many degrees of freedom during the time evolution and cannot be restored by local measurements¹¹. This process i.e., the loss of information through delocalization is called scrambling^{12,13}. In systems, where the short time exponential growth, bounded by thermal Lyapunov exponent $\lambda_L \leq 2\pi k_B T$ ^{2,14,15} is present are called fast scramblers, but there are also models where this short time growth is absent, called slow scramblers. Thus, a possible way to understand the nature of chaos and

test capabilities of condensed matter systems for quantum information processing is to investigate the temporal behavior of OTOC. It has already been analyzed in a variety of systems, including Luttinger liquids¹⁶, random unitary circuits^{17–19} in quantum Ising chain²⁰, XY chains²¹, conformal field theories^{22,23} and Sachdev-Ye-Kitaev model^{24–26}. OTOC has been investigated experimentally as well in different many-body systems such as in cold atomic systems, trapped ions or in a nuclear magnetic resonance quantum simulator^{27–33}.

In this paper, we consider Dirac–Weyl systems in one, two and three dimensions, characterized by linear energy-momentum relation. These models are popular not only in the condensed matter physics but possess a rich history in high energy physics as well³⁴. As already mentioned, the common property of these systems is the linear energy-momentum dispersion relation and the Brillouin zone contains monopole-like structures called Weyl or Dirac nodes. The most famous descendants are carbon nanotubes in one, graphene in two and Weyl-semimetals in three dimensions^{35,36}, respectively. The low energy excitations are described by massless non-interacting fermions and one of their unique features is that they can host topologically non-trivial states which are robust against small perturbations^{35,37,38}. This non-trivial topology shows up in exotic electromagnetic transport phenomena such as topologically protected edge states in zigzag carbon nanotubes in presence of spin-orbit interaction³⁷, the quantum spin Hall effect in graphene³⁹ or the chiral anomaly^{40,41} or the anomalous Hall conductivity in Weyl semimetals⁴².

To obtain the short and late time behavior of the OTOC, we rewrite Eq. (1) in a more suggestive way as

$$C(t) = -\langle [W(t), V(0)] \rangle^2 + K(t) \quad (2)$$

where the first term is the square of the expectation value of the spin commutator and $K(t)$ is the variance of the commutator, i.e. $K(t) = \langle [W(t), V(0)]^2 \rangle - \langle [W(t), V(0)] \rangle^2$. In other words, $K(t)$ measures the spreading of the probability distribution of the commutator compared to its expectation value. When the commutator as an operator is a c-number, the variance is zero¹⁶ which means the distribution of the commutator is a Dirac-delta function. A finite variance is the first indicator of the broadening of the distribution around the mean value. In our case, this indicates how the OTOC, i.e. the expectation value of the square of the commutator differs from the square of the expectation value of the commutator. One can in principle also obtain the full counting statistics of the commutator in general by calculating higher moments as $\langle [W(t), V(0)]^n \rangle$ in a similar way as in Eq. (1).

In this work, we investigate the short and late time behavior of OTOC in Dirac-Weyl systems. In this context, the OTOC was already investigated in interacting graphene⁴³ Weyl semimetals⁴⁴ from different approaches. We are focusing on the response of a single non-interacting Dirac-Weyl cone which is diagonalizable straightforwardly, thus integrable. The short time behavior of OTOC gives a universal t^2 initial rise from both the square of the expectation value of the commutator and the variance from Eq. (2), though the contribution of the former parametrically is dominant over the latter. The late time decay is dominated only by $K(t)$ and depends on the dimension of the system and is independent of the chemical potential.

This paper is organized as follows: in Sec. II, we introduce the model Hamiltonian and the operators used for further calculations. In Sec. III, the time-dependent expectation value of the spin commutator is calculated by separating the matrix element and occupation number dependent parts. In Sec. IV calculation procedure of OTOC is outlined and briefly discuss the results. In Sec. V, our main results are summarized.

II. LOW ENERGY EFFECTIVE HAMILTONIAN

The low energy effective Hamiltonian of Dirac-Weyl systems in d dimension is given by

$$H = v_F \mathbf{p} \cdot \boldsymbol{\sigma} \quad (3)$$

where \mathbf{p} is the momentum operator, v_F is the Fermi velocity and $\boldsymbol{\sigma}$ denotes the corresponding Pauli matrices. For $d = 1$ only σ_x appears in the Hamiltonian, for $d = 2$, $\boldsymbol{\sigma} = [\sigma_x, \sigma_y]$ and for three dimensions all Pauli matrices are present. At low energy, the energy dispersion relation is linear in momentum for any dimension: $\varepsilon_\lambda(\mathbf{k}) = \lambda \hbar v_F |\mathbf{k}|$ with $\lambda = \pm$ the band index^{35,36}. The corresponding wavefunctions are written as

$$\phi_{\lambda, \mathbf{k}}(\mathbf{r}) = \frac{1}{\sqrt{V_d}} e^{i\mathbf{k}\mathbf{r}} |k, \lambda\rangle, \quad (4)$$

where V_d is the volume and $|k, \lambda\rangle$ is the normalized eigen-spinor written in d dimension as

$$|k, \lambda\rangle = \begin{cases} \frac{1}{\sqrt{2}} \begin{bmatrix} 1 \\ \lambda \end{bmatrix} & \text{for } d = 1, \\ \frac{1}{\sqrt{2}} \begin{bmatrix} \lambda \\ e^{i\varphi_k} \end{bmatrix} & \text{for } d = 2, \\ \begin{bmatrix} \cos\left(\frac{\vartheta_k + (\lambda-1)\pi/2}{2}\right) \\ \sin\left(\frac{\vartheta_k + (\lambda-1)\pi/2}{2}\right) e^{i\varphi_k} \end{bmatrix} & \text{for } d = 3. \end{cases} \quad (5)$$

Here φ_k is the polar angle in two and the azimuthal angle in three dimensions and ϑ_k is the polar angle in 3D. Using Eq. (4), we construct the local field operators. Considering a Hermitian operator \mathcal{O} , the spatial and time dependent formula in second quantized formalism is given by⁴⁵

$$\mathcal{O}(\mathbf{r}, t) = \frac{1}{V_d} \sum_{k_1, k_2} e^{i(\mathbf{k}_1 - \mathbf{k}_2)\mathbf{r}} T(k_1, k_2) \langle k_2 | \mathcal{O} | k_1 \rangle c_{k_2}^\dagger c_{k_1}. \quad (6)$$

Here, $k_i = (\mathbf{k}_i, \lambda_i)$ is a combination of the momentum state and band index, and $c_{k_2}^\dagger$ and c_{k_1} are fermionic creation and annihilation operators into state k_2 and k_1 , respectively. The time dependence is represented by $T(k_1, k_2) = \exp[i(\varepsilon_{\lambda_2}(\mathbf{k}_2) - \varepsilon_{\lambda_1}(\mathbf{k}_1))t]$ with $\varepsilon_{\lambda_i}(\mathbf{k}_i)$, the energy of the Dirac-Weyl fermions and $\langle k_2 | \mathcal{O} | k_1 \rangle$ is the corresponding matrix element of \mathcal{O} operator. In the following sections, we are focusing on the expectation value of the spin commutators and the corresponding OTOC for spatially identical spin operators, thus we set $\mathbf{r} = 0$ in Eq. (6) during the calculations.

III. SPIN CORRELATION FUNCTION

The correlation function of two spin operators $\sigma_\alpha(0, t)$ are related to linear response and defined by the standard Kubo formula as⁴⁶

$$\Pi^{\alpha\beta}(t) = i \langle [\sigma_\alpha(0, t), \sigma_\beta(0, 0)] \rangle \Theta(t). \quad (7)$$

Here, $\Theta(t)$ is the Heaviside step function and $\alpha, \beta = x, y, z$. For diagonal case, when $\alpha = \beta$ the expectation value of the commutator is

$$\Pi^{\alpha\alpha}(t) = \frac{i}{V_d^2} \sum_{k_1, k_2} T(k_1, k_2) |\langle k_2 | \sigma_\alpha | k_1 \rangle|^2 [f(k_2) - f(k_1)], \quad (8)$$

for $t > 0$ and $f(k_i) = [\exp((\varepsilon_{\lambda_i}(\mathbf{k}_i) - \mu)/k_B T) + 1]^{-1}$ is the Fermi function. Eq. (8) consists of two terms, the occupation number dependent part and the absolute value square of the matrix elements. These two terms are treated separately in the followings.

A. Matrix elements

By rewriting the appropriate polar and azimuthal coordinates of the eigenspinors in Eq. (5) to Cartesian coordinates of momentum vector, the square of matrix elements in Eq. (8) has a closed formula in d dimension given by

$$|\langle k_2 | \sigma_\alpha | k_1 \rangle|^2 = \frac{1}{2} \left[1 - \lambda_1 \lambda_2 \frac{\mathbf{k}_1 \mathbf{k}_2 - 2k_{1,\alpha} k_{2,\alpha}}{|\mathbf{k}_1| |\mathbf{k}_2|} \right]. \quad (9)$$

In one dimension, there are no angular integrals and Eq. (9) gives only Kronecker delta function as: $|\langle k_2 | \sigma_x | k_1 \rangle|^2 = \delta_{\lambda,\lambda'}$ and $|\langle k_2 | \sigma_{y,z} | k_1 \rangle|^2 = 1 - \delta_{\lambda,\lambda'}$. Rewriting the summations into spherical integrals in Eq. (8), we evaluate the angular integrals separately since only the square of matrix elements in Eq. (9) depends on angular variables and are independent from the absolute value of momentum. In two and three dimensions, the integrals over angular variables are

$$M_d^\alpha(k_1, k_2) = \int \frac{d\Omega_1 d\Omega_2}{(2\pi)^{2(d-1)}} |\langle k_2 | \sigma_\alpha | k_1 \rangle|^2, \quad (10)$$

where $d\Omega_i = d\varphi_{k_i}$ in two and $d\Omega_i = d\varphi_{k_i} \sin(\vartheta_{k_i}) d\vartheta_{k_i}$ in three dimensions with $i = 1, 2$. In one dimension, there is no angular integral, but we can still introduce $M_1^\alpha(k_1, k_2)$ by changing the boundary of the momentum integrals from $(-\infty, \infty)$ to $[0, \infty)$. Evaluating the integrals, we end up with

$$M_1^\alpha(k_1, k_2) = 2, \quad M_2^\alpha(k_1, k_2) = \frac{1}{2}, \quad M_3^\alpha(k_1, k_2) = \frac{2}{(2\pi)^2}. \quad (11)$$

The angular integral of the square of matrix elements yields a band index (λ) independent constant what we use in the next section to derive the time dependence of the expectation value of the commutator.

B. Explicit form of the expectation value of the commutator

We evaluate the remaining integrals over the radial component of momentum. Let us introduce the following functions as

$$G_d^<(t) = \frac{1}{2\pi} \sum_{\lambda_1} \int_0^\infty dk \, k^{d-1} T(k_1, 0) f(k_1) e^{-\delta k} \quad (12)$$

$$G_d^>(t) = \frac{1}{2\pi} \sum_{\lambda_1} \int_0^\infty dk \, k^{d-1} T(k_1, 0) (1 - f(k_1)) e^{-\delta k}. \quad (13)$$

Here, dk denotes the integral over the radial component of the momentum and δ is the exponential cutoff which is a commonly used cutoff scheme in field theories⁴⁶. The functions defined in Eqs. (12) and (13) are practically the greater and lesser Greens functions^{45,47} with the only difference that instead of summing over the full momentum space, only the radial component is integrated over.

We express the expectation value of the commutator in terms of these Green's functions as

$$\Pi^{\alpha\alpha}(t) = -2M_d^\alpha(k_1, k_2) \text{Im} [G_d^>(t) \bar{G}_d^<(t)]. \quad (14)$$

We are interested in the zero temperature limit, allowing us to substitute the Fermi function with a Heaviside step function. In these non-interacting systems, no exponential growth with thermal Lyapunov exponent is expected, which justifies this simplification. The integral defined in the Green's functions can be evaluated, the detailed derivation is presented in Appendix A. After some straightforward algebra, the commutator looks as

$$\Pi^{\alpha\alpha}(\tau) = \text{sgn}(\mu) \times \begin{cases} \frac{8}{(2\pi)^2 \delta^2} \frac{e^{-\nu}}{(\tau^2 + 1)^2} [\sin(\nu\tau) + \tau \cos(\nu\tau)] & \text{for } d = 1, \\ \frac{2e^{-\nu}}{(2\pi)^2 \delta^4} \frac{\tau^2 - 1}{(\tau^2 + 1)^4} [((1 - \nu)\tau^2 - (1 + \nu)) \sin(\nu\tau) - \tau (\nu\tau^2 + (2 + \nu)) \cos(\nu\tau)] & \text{for } d = 2, \\ \frac{16e^{-\nu}}{(2\pi)^4 \delta^6} \frac{3\tau^2 - 1}{(\tau^2 + 1)^6} [\nu(2 - \nu)\tau^4 + (6 - 2\nu^2)\tau^2 - (\nu^2 + 2\nu + 2)] \sin(\nu\tau) - \\ - [\nu^2\tau^5 - (2\nu^2 + 4\nu - 2)\tau^3 + (\nu^2 + 4\nu + 6)\tau] \cos(\nu\tau) & \text{for } d = 3. \end{cases} \quad (15)$$

Here, we introduced dimensionless variable for time as

$\tau = v_F t / \delta$ and $\nu = |\mu| \delta / v_F$ for chemical potential with

v_F/δ , the high energy cutoff.

The spin correlation functions with respect to time can be separated into three distinct regions: short time growth for $\tau \ll 1$, an intermediate time window for $1 \ll \tau \ll 1/\nu$ and the late time decay when $\tau \gg 1/\nu$. Since the chemical potential always lies below the high energy cutoff, we use $\nu \ll 1$.

For short times, the correlation function grows linearly with time in all considered dimension. This short time linear behavior is shown in Fig. 1. The intermediate time window which also represents the late time decay for the $\nu = 0$ case is depicted in Fig. 1. The exponents of power-law decay can be obtained by calculating the asymptotic behavior of the rational function in Eq. (15) and taking the $\nu\tau \rightarrow 0$ for the trigonometric terms. As a result, the decay in d dimensions is given by $\sim \tau^{-(2d+1)}$. For the third case with $\tau \gg 1/\nu$, the asymptotic behavior is obtained as $\sim \nu^{d-1} \cos(\nu\tau)/\tau^{(2(d-1)!+1)}$ with ! denoting the factorial function. We collected the short, intermediate and late time behaviors of the expectation value of the spin-spin commutator in Table I and displayed them in Fig. 1.

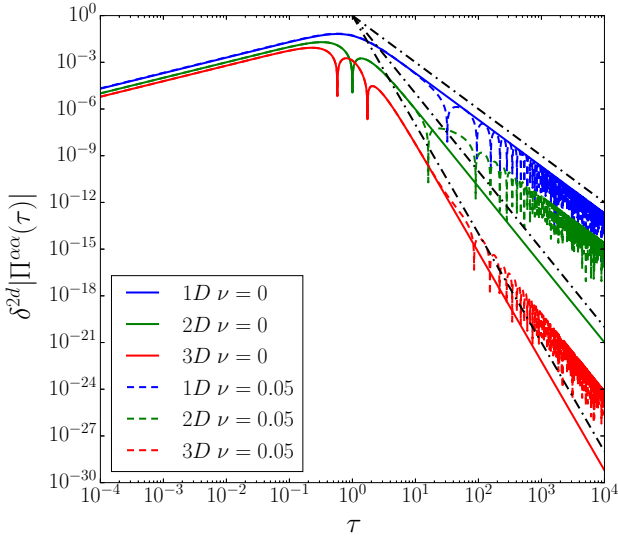


FIG. 1. The temporal dynamics of the spin commutator in one (red), two (green) and three (blue) dimensions is plotted. The solid and dashed lines represent the $\nu = 0$ and $\nu = 0.05$ case, respectively. In any dimension, the early time growth scales with τ . For intermediate times, the temporal decay exponent differs from the late time exponent for $d = 2$ and 3 , which is apparent in the intermediate time window. For late times, the response decays as a power-law whose exponent depends on the chemical potential and the dimension. The black dash-dotted lines are τ^{-3} , τ^{-5} and τ^{-7} representing the possible intermediate and late time decay, respectively.

IV. OUT-OF-TIME-ORDERED COMMUTATOR

The Dirac–Weyl systems are simple integrable models, thus OTOC is expected to display a $\sim t^2$ initial growth and a power-law decay for late times. Using Eq. (1), the OTOC for spatially non-separated spin operators is given by

$$C_{\alpha\alpha}(t) = -\frac{1}{V^4} \sum_{\substack{k_1, k_2, \\ k_3}} \sum_{\substack{l_1, l_2, \\ l_3}} T(k_1, k_2) T(l_1, l_2) \times \\ \times [\langle k_2 | \sigma_\alpha | k_1 \rangle \langle k_1 | \sigma_\alpha | k_3 \rangle \langle l_2 | \sigma_\alpha | l_1 \rangle \langle l_1 | \sigma_\alpha | l_3 \rangle \langle a_{k_2}^\dagger a_{k_3} a_{l_2}^\dagger a_{l_3} \rangle \\ - \langle k_2 | \sigma_\alpha | k_1 \rangle \langle k_1 | \sigma_\alpha | k_3 \rangle \langle l_2 | \sigma_\alpha | l_1 \rangle \langle l_3 | \sigma_\alpha | l_2 \rangle \langle a_{k_2}^\dagger a_{k_3} a_{l_3}^\dagger a_{l_1} \rangle \\ - \langle k_2 | \sigma_\alpha | k_1 \rangle \langle k_3 | \sigma_\alpha | k_2 \rangle \langle l_2 | \sigma_\alpha | l_1 \rangle \langle l_1 | \sigma_\alpha | l_3 \rangle \langle a_{k_3}^\dagger a_{k_1} a_{l_2}^\dagger a_{l_3} \rangle \\ + \langle k_2 | \sigma_\alpha | k_1 \rangle \langle k_3 | \sigma_\alpha | k_2 \rangle \langle l_2 | \sigma_\alpha | l_1 \rangle \langle l_3 | \sigma_\alpha | l_2 \rangle \langle a_{k_3}^\dagger a_{k_1} a_{l_3}^\dagger a_{l_1} \rangle]. \quad (16)$$

Here, $\alpha = x, y, z$ denotes the component of the spin. By using Wick's theorem, the expectation value of four fermionic operators is

$$\langle a_{k_1}^\dagger a_{k_2} a_{k_3}^\dagger a_{k_4} \rangle = \delta_{k_1, k_2} \delta_{k_3, k_4} f(k_1) f(k_3) \\ + \delta_{k_1, k_4} \delta_{k_3, k_2} f(k_1) [1 - f(k_3)]. \quad (17)$$

The commutator can be split into two parts, the first and second one containing $f(k_i)f(l_j)$ and $f(k_i)[1 - f(l_j)]$ terms, respectively. The first part gives the square of the expectation value of the commutator, defined in Eq. (8), thus the OTOC looks as

$$C_{\alpha\alpha}(t) = -\langle [\sigma_\alpha(t), \sigma_\alpha] \rangle^2 + K_{\alpha\alpha}(t), \quad (18)$$

where $K_{\alpha\alpha}(t)$ is the variance of the commutator. It is given by

$$K_{\alpha\alpha}(t) = -\frac{1}{V^4} \sum_{\substack{k_1, k_2, \\ l_1, l_2}} \langle k_2 | \sigma_\alpha | k_1 \rangle \langle k_1 | \sigma_\alpha | l_2 \rangle \times \\ \times \langle l_2 | \sigma_\alpha | l_1 \rangle \langle l_1 | \sigma_\alpha | k_2 \rangle \times \\ \times \left(T(k_1, k_2) T(l_1, l_2) [f(k_2)[1 - f(l_2)] + f(k_1)[1 - f(l_1)]] \right. \\ \left. - T(k_1, l_1) [f(k_2)(1 - f(l_2)) + f(l_2)(1 - f(k_2))] \right). \quad (19)$$

	$\tau \ll 1$	$1 \ll \tau \ll 1/\nu$	$\tau \gg 1/\nu$
1D	τ	τ^{-3}	$\cos(\nu\tau)/\tau^3$
2D	τ	τ^{-5}	$\nu \cos(\nu\tau)/\tau^3$
3D	τ	τ^{-7}	$\nu^2 \cos(\nu\tau)/\tau^5$

TABLE I. The short, intermediate and late time behavior of the spin-spin correlation function are summarized.

The product of the matrix elements is treated separately from remaining terms, and the integral over the angular variables, denoted by $N_d^\alpha(k_1, k_2)$ gives

$$N_d^\alpha(k_1, k_2) = \frac{(M_d^\alpha(k_1, k_2))^2}{2}, \quad (20)$$

where $M_d^\alpha(k_1, k_2)$ is defined in Eq. (11). The remaining terms depend only the radial component of the momentum. Using Eq. (12) and Eq. (13), we can rewrite the

variance in Eq. (19) as

$$K_{\alpha\alpha}(t) = 2N_d^\alpha \left(|G_d^>(t) + G_d^<(t)|^2 \left(\text{Re} [G_d^>(0^+) \bar{G}_d^<(0^+)] - \text{Re} [G_d^>(t) \bar{G}_d^<(t)] \right) - 2 \left(\text{Im} [G_d^>(t) \bar{G}_d^<(t)] \right)^2 \right). \quad (21)$$

Here $G_d^{</>}(0^+) = \lim_{t \rightarrow 0^+} G_d^{</>}(t)$ and N_d^α is the prefactor coming from Eq. (20). The detailed derivation is presented in Appendix A. Evaluating the integrals yields the variance as

$$K_{\alpha\alpha}(\tau) = \begin{cases} \left[\frac{16}{(2\pi)^4 \delta^4} \frac{e^{-\nu}}{(\tau^2 + 1)^2} \left[(2 - e^{-\nu}) + \frac{e^{-\nu}}{\tau^2 + 1} - 2 \frac{e^{-\nu} (\tau \cos(\nu\tau) + \sin(\nu\tau))^2 + \cos(\nu\tau) - \tau \sin(\nu\tau)}{(\tau^2 + 1)^2} \right] \right] & \text{for } d = 1, \\ \left[\frac{e^{-\nu}}{(2\pi)^4 \delta^8} \frac{(\tau^2 - 1)^2}{(\tau^2 + 1)^4} \left[((2 - e^{-\nu}(1 + \nu))(1 + \nu) + \frac{e^{-\nu}((1 + \nu)^2 + (\nu\tau)^2)}{(\tau^2 + 1)^2} - \frac{2}{(\tau^2 + 1)^4} [(\tau^2 - 1)[((1 - \nu)\tau^2 - (1 + \nu)) \cos(\nu\tau) + \tau(\nu\tau^2 + (2 + \nu)) \sin(\nu\tau)] + e^{-\nu} [\tau(\nu\tau^2 + (2 + \nu)) \cos(\nu\tau) - ((1 - \nu)\tau^2 - (1 + \nu)) \sin(\nu\tau)]^2] \right] \right] & \text{for } d = 2, \\ \left[\frac{64}{(2\pi)^8 \delta^{12}} \frac{e^{-\nu}(3\tau^2 - 1)^2}{(\tau^2 + 1)^6} \left[(2 + 2\nu + \nu^2)(4 - e^{-\nu}(2 + 2\nu + \nu^2)) + \frac{e^{-\nu}((\nu^2\tau^2 - (2 + 2\nu + \nu^2))^2 + 4(\nu(\nu + 1)\tau)^2)}{(\tau^2 + 1)^3} - \frac{2}{(\tau^2 + 1)^6} [2(3\tau^2 - 1)[\nu(2 - \nu)\tau^4 + (6 - 2\nu^2)\tau^2 - (\nu^2 + 2\nu + 2)] \cos(\nu\tau) + [\nu^2\tau^5 - (2\nu^2 + 4\nu - 2)\tau^3 + (\nu^2 + 4\nu + 6)\tau] \sin(\nu\tau)] + e^{-\nu} [\nu^2\tau^5 - (2\nu^2 + 4\nu - 2)\tau^3 + (\nu^2 + 4\nu + 6)\tau] \cos(\nu\tau) - [\nu(2 - \nu)\tau^4 + (6 - 2\nu^2)\tau^2 - (\nu^2 + 2\nu + 2)] \sin(\nu\tau)]^2 \right] \right] & \text{for } d = 3. \end{cases} \quad (22)$$

Here, we used again the dimensionless variables for time (τ) and the chemical potential (ν).

Eq. (22) allows us to investigate the short and late time behavior of the OTOC, similarly to the case of the commutator in Eq. (15). The natural energy scales in the problem are μ and v_F/δ , translating into three separate temporal windows for short, intermediate and late times as $\tau \ll 1$, $1 \ll \tau \ll 1/\nu$ and $1/\nu \ll \tau$, respectively. For short times, the OTOC grows with τ^2 also shown in Fig. 2. This behavior follows from a Baker-Campbell-Hausdorff expansion of $\sigma_\alpha(t)$ with the nested commutators^{2,16}

$$\sigma_\alpha(t) = \sigma_\alpha + it[H, \sigma_\alpha] + \frac{(it)^2}{2!} [H, [H, \sigma_\alpha]] + \dots \quad (23)$$

The contribution of the first term in Eq. (23) gives trivially vanishing contribution to both the expectation value of the commutator and the OTOC. The τ^2 growth arises from the second term in Eq. (23) with the coefficient

$\langle [[H, \sigma_\alpha], \sigma_\alpha]^2 \rangle$. This short time growth originates from both the square of the expectation value of the commutator and the variance of the commutator in Eq. (22).

We note that the second term in Eq. (23) is also responsible for the linear growth of the response function for short times and it ensures that both the linear response and the OTOC have to be real since H and σ_α are Hermitian operators, thus the expectation value of their commutator has to be real.

For intermediate and late times, the OTOC decays in an identical power-law fashion, shown in Fig. 2. Irrespective of the value of ν , the asymptotics of the temporal decay is $\sim \tau^{-4(d-1)!}$ with ! denoting the factorial function which is the same result as we obtained for late times. This means the exponent of the power-law decay is independent of the chemical potential and depends only on the spatial dimension of the system. This behavior comes from the time-independent part of Eq. (21) i.e., $\text{Re} [G_d^>(0^+) \bar{G}_d^<(0^+)]$. The short and late time behaviors

are represented in Table II.

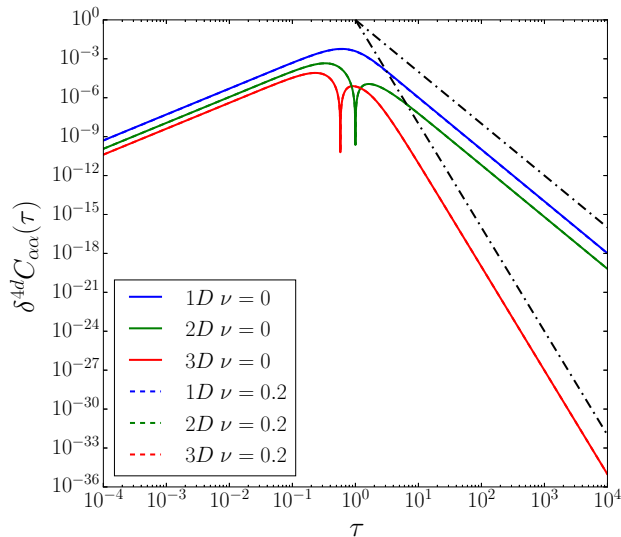


FIG. 2. Short, intermediate and late time behavior of the OTOC in one (blue), two (green) and three (red) dimensions. The solid and dashed lines represent the $\nu = 0$ and $\nu = 0.2$ case, respectively. For short times, OTOC exhibits τ^2 growth with a chemical potential dependent prefactor. For intermediate and late times it decays as a power-law with an exponent depending only on the spatial dimension. In contrast with the correlation function, there is no difference in the decay for intermediate and late times. The black dash-dotted lines are τ^{-4} and τ^{-8} functions.

The influence of the variance on OTOC is plotted in Fig. 3. For short times, both the square of expectation value of the commutator and the variance scales with τ^2 but former parametrically is dominant over the latter. This can be seen in Fig. 3 since the $K_{\alpha\alpha}(\tau)/C_{\alpha\alpha}(\tau)$ ratio is small for $\tau \ll 1$. For intermediate and late times, the ratio tends to one, independently of the chemical potential, indicating that the OTOC is dominated by the variance in this regime.

In general, the quantum butterfly effect shows up in systems with exponential growth of the OTOC at short times and a large late time value^{2,14,48}. For non-interacting Dirac-Weyl systems, the OTOC scales with τ^2 initially, i.e. with the lowest possible power and no exponential growth is identified. The late time OTOC vanishes which agrees with the general expectations since our

	$\tau \ll 1$	$\tau \gg 1$
1D	τ^2	τ^{-4}
2D	τ^2	τ^{-4}
3D	τ^2	τ^{-8}

TABLE II. Characteristic time dependence of OTOC for short, intermediate and late times. For the latter two, the behaviour is identical, though.

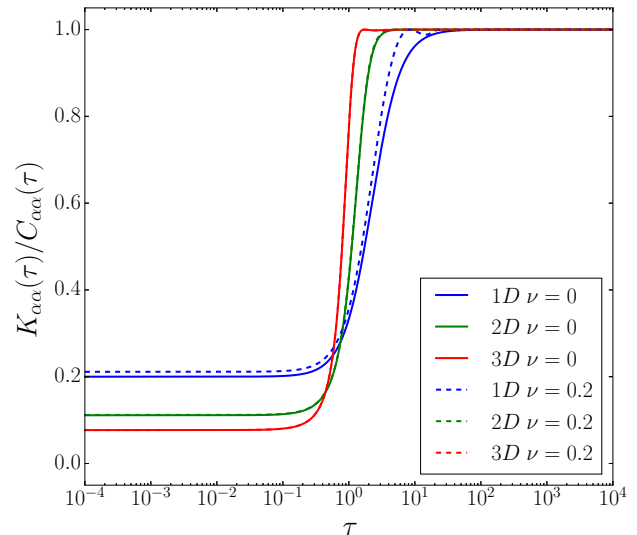


FIG. 3. Ratio of the variance and OTOC as a function of time. The solid and dashed lines represent the $\nu = 0$ and $\nu = 0.2$ case, respectively. For $\tau \ll 1$, the main contribution to OTOC comes from the square of the expectation value of the commutator, while when $\tau \gg 1$ the variance dominates.

models are non-interacting without any chaotic feature. This means the information encoded in local operators is lost slowly through time evolution^{49,50}. The same short time behavior was identified in different integrable models like Heisenberg XXZ chain¹⁶, quantum Ising chain²⁰, and XY chain²¹. These models also exhibit late time power-law decay, similarly to our findings, though the exponents depend on the actual system.

V. SUMMARY

In this work, we have investigated dynamics of the expectation value of the spin commutators and the corresponding OTOC in Dirac-Weyl systems in $d = 1, 2$ and 3 dimensions. Three distinct temporal regions are identified during time evolution. For short times, $\tau \ll 1$, we obtain a linear initial rise in time. For intermediate times, when $1 \ll \tau \ll 1/\nu$ the expectation value of the commutator starts to decay with power-law as $\sim \tau^{-(2d+1)}$. In the late time regime, the commutator decays with $\sim \nu^{d-1} \cos(\nu\tau)/\tau^{(2(d-1)!+1)}$ for finite doping.

The OTOC of local spin operators displays robust behavior, mostly independent of chemical potential. For short times, the OTOC grows with τ^2 , the lowest possible power, while for late times, it decays with $\tau^{-(4(d-1)!)}$ for all spin components. We note that the decay in the intermediate time window coincides with that for late times. The short time behavior is determined by both the square of the expectation value of the commutator

and the variance while for late times the variance gives the dominant part. The power-law growth for short times and the vanishing late time value indicate that these systems are slow information scramblers. These results are essential when the effect of other sources of information scrambling (interaction, disorder) are analyzed on top of the non-interacting results.

ACKNOWLEDGMENTS

This research is supported by the National Research, Development and Innovation Office - NKFIH within the Quantum Technology National Excellence Program (Project No. 2017-1.2.1-NKP-2017-00001) and K119442, SNN118028 and by the BME-Nanotechnology FIKP grant of EMMI (BME FIKP-NAT) and by Romanian UEFISCDI, project number PN-III-P4-ID-PCE-2016-0032 and by the NKP-19-3 New National Excellence Program of the Ministry for Innovation and Technology

Appendix A: Derivation of variance for the OTOC

To obtain the expectation value of the spin commutator and the OTOC, first, we evaluate the integrals defined by $G_d^{</>}(t)$ in Eqs. (12) and (13). We focus on the zero temperature case in one dimension but higher-dimensional extensions are straightforward. It looks as

$$G_1^<(t) = \sum_{\lambda} \int_0^{\infty} \frac{dk}{2\pi} e^{-i\lambda v_F k(t - \lambda i\delta)} \Theta(\mu - \varepsilon_{\lambda}(k)), \quad (\text{A1})$$

$$G_1^>(t) = \sum_{\lambda} \int_0^{\infty} \frac{dk}{2\pi} e^{-i\lambda v_F k(t - \lambda i\delta)} (1 - \Theta(\mu - \varepsilon_{\lambda}(k))). \quad (\text{A2})$$

Evaluating the integrals and using the dimensionless variables, we end up with

$$G_1^<(\tau) = \frac{1}{2\pi\delta} \left[\frac{ie^{-i\nu\tau}e^{-\nu}}{\tau - i} + \frac{2}{\tau^2 + 1} \right], \quad (\text{A3})$$

$$G_1^>(\tau) = \frac{1}{2\pi\delta} \frac{-ie^{-i\nu\tau}e^{-\nu}}{\tau - i}. \quad (\text{A4})$$

The variance term of OTOC can be expressed with $G_d^{</>}(t)$ similarly to the correlation function in Eq. (14). Rewriting the wavevector integral with spherical coordinates, we can separate the angular integrals since the matrix elements are not containing the radial part of the integral variables. Integrating over the matrix elements gives N_d^{α} in Eq. (20) which is independent from the band indices. The remaining parts are the Fermi function and the terms containing time evolution which are depending on the band index and the radial component of the momentum vector through the energy. These terms of Eq. (19) can be split into two parts as

$$I_1 = T(k_1, k_2)T(l_1, l_2)(f(k_2)[1 - f(l_2)] + f(k_1)[1 - f(l_1)]) \quad (\text{A5})$$

$$I_2 = T(k_1, l_1)[f(k_2)(1 - f(l_2)) + f(l_2)(1 - f(k_2))] \quad (\text{A6})$$

Since I_1 contains product of two time dependent terms and products of Fermi functions, we rewrite it as

$$I_1 = -T(k_1, k_2)T(l_1, l_2)[f(k_2) - f(k_1)][f(l_2) - f(l_1)] + T(k_1, k_2)T(l_1, l_2)[f(k_2)(1 - f(l_1)) + f(k_1)(1 - f(l_2))] \quad (\text{A7})$$

If we integrate over the radial component of the momentum and make the summations over the band indices the result matches with the square of radial integrals in the commutator in Eq. (8). The integral of second time evolution containing term in Eq. (A7) is also traced back to product of Green's functions. Thus the summation over the band indices and the integrals of I_1 is written with the Green's functions as

$$\begin{aligned} & \sum_{\substack{\lambda_1, \lambda_2, \\ \mu_1, \mu_2}} \int_0^{\infty} \frac{dk_1}{2\pi} \int_0^{\infty} \frac{dk_2}{2\pi} \int_0^{\infty} \frac{dl_1}{2\pi} \int_0^{\infty} \frac{dl_2}{2\pi} \times \\ & \quad \times k_1^{d-1} k_2^{d-1} l_1^{d-1} l_2^{d-1} I_1 = \\ & - (2i\text{Im} [G_d^>(t)\bar{G}_d^<(t)])^2 + 2\text{Re} [G_d^>(t)\bar{G}_d^<(t)] \times \\ & \quad \times \sum_{\lambda_1, \mu_2} \int_0^{\infty} \frac{dk_1}{2\pi} \int_0^{\infty} \frac{dl_2}{2\pi} k_1^{d-1} l_2^{d-1} T(k_1, l_2). \end{aligned} \quad (\text{A8})$$

We swapped variables in the last term of Eq. (A7). The remaining two integrals gives the same result as $|G_d^>(t) + G_d^<(t)|^2$.

The formula of I_2 in Eq. (A6) resembles closely to the second term of Eq. (A7) except it has only one time dependent part. Thus, if we multiply it with $\lim_{t \rightarrow 0^+} T(k_2, l_2)$ which is 1 we get the same structure as in Eq. (A7). This implies that the result is the same as the last term of Eq. (A8) after the integrals and summations. Taking the $t \rightarrow 0^+$ limit, we end up with the last term of Eq. (19) expressed with Green's functions as

$$\begin{aligned} & \sum_{\substack{\lambda_1, \lambda_2, \\ \mu_1, \mu_2}} \int_0^{\infty} \frac{dk_1}{2\pi} \int_0^{\infty} \frac{dk_2}{2\pi} \int_0^{\infty} \frac{dl_1}{2\pi} \int_0^{\infty} \frac{dl_2}{2\pi} \times \\ & \quad \times k_1^{d-1} k_2^{d-1} l_1^{d-1} l_2^{d-1} I_2 = \\ & 2 |G_d^>(t) + G_d^<(t)|^2 \text{Re} [G_d^>(0^+)\bar{G}_d^<(0^+)] \end{aligned} \quad (\text{A9})$$

Substituting the result of (A8) and (A9) into Eq. (19) and multiply it with N_d^{α} from the angular integrals, we

obtain the variance with the Green's functions in Eq. (21). By inserting the explicit formula of the correspond-

ing Green's function, we obtain the complete time dependence of the OTOC.

* okvatovity@phy.bme.hu

- ¹ J. Steinberg and B. Swingle, Physical Review D **99**, 076007 (2019).
- ² D. A. Roberts and B. Swingle, Physical Review Letters **117**, 091602 (2016).
- ³ J. S. Cotler, G. Gur-Ari, M. Hanada, J. Polchinski, P. Saad, S. H. Shenker, D. Stanford, A. Streicher, and M. Tezuka, Journal of High Energy Physics **05**, 118 (2017).
- ⁴ X. Chen and T. Zhou (2018), arXiv:1804.08655.
- ⁵ O. Bohigas, M. J. Giannoni, and C. Schmit, Physical Review Letters **52**, 1 (1984).
- ⁶ M. Srednicki, Physical Review E **50**, 888 (1994).
- ⁷ J. M. Deutsch, Physical Review A **43**, 2046 (1991).
- ⁸ T. Prosen and I. Pižorn, Physical Review A **76**, 032316 (2007).
- ⁹ K. Hashimoto, K. Murata, and R. Yoshii, Journal of High Energy Physics **2017**, 10 (2017).
- ¹⁰ A. Larkin and Y. N. Ovchinnikov, Sov. Phys. JETP **28**, 1200 (1969).
- ¹¹ D. N. Page, Physical Review Letters **71**, 1291 (1993).
- ¹² N. Lashkari, D. Stanford, M. Hastings, T. Osborne, and P. Hayden, Journal of High Energy Physics **4**, 22 (2013).
- ¹³ Y. Sekino and L. Susskind, Journal of High Energy Physics **2008**, 10 (2008).
- ¹⁴ J. Maldacena, S. H. Shenker, and D. Stanford, Journal of High Energy Physics **08**, 106 (2016).
- ¹⁵ N. Tsuji, T. Shitara, and M. Ueda, Physical Review E **98**, 012216 (2018).
- ¹⁶ B. Dóra and R. Moessner, Physical Review Letters **119**, 026802 (2017).
- ¹⁷ A. Nahum, S. Vijay, and J. Haah, Physical Review X **8**, 021014 (2018).
- ¹⁸ T. Rakovszky, F. Pollmann, and C. von Keyserlingk, Physical Review X **8**, 031058 (2018).
- ¹⁹ C. von Keyserlingk, T. Rakovszky, F. Pollmann, and S. Sondhi, Physical Review X **8**, 021013 (2018).
- ²⁰ C.-J. Lin and O. I. Motrunich, Physical Review B **97**, 144304 (2018).
- ²¹ J. Bao and C.-Y. Zhang (2019), arXiv:1901.09327v2.
- ²² D. A. Roberts, D. Stanford, and L. Susskind, Journal of High Energy Physics **3**, 51 (2015).
- ²³ D. Stanford, Journal of High Energy Physics **10**, 009 (2016).
- ²⁴ S. Sachdev and J. Ye, Physical Review Letters **70**, 3339 (1993).
- ²⁵ J. Maldacena and D. Stanford, Physical Review D **94**, 106002 (2016).
- ²⁶ N. Tsuji, P. Werner, and M. Ueda, Physical Review A **95**, 011601 (2017).
- ²⁷ J. Li, R. Fan, H. Wang, B. Ye, B. Zeng, H. Zhai, X. Peng, and J. Du, Physical Review X **7**, 031011 (2017).
- ²⁸ B. Swingle, G. Bentsen, M. Schleier-Smith, and P. Hayden, Physical Review A **94**, 040302 (2016).
- ²⁹ G. Zhu, M. Hafezi, and T. Grover, Physical Review A **94**, 062329 (2016).
- ³⁰ A. M. Kaufman, M. E. Tai, A. Lukin, M. Rispoli, R. Schittko, P. M. Preiss, and M. Greiner, Science **353**, 6301 (2016).
- ³¹ M. Gärttner, J. G. Bohnet, A. Safavi-Naini, M. L. Wall, J. J. Bollinger, and A. M. Rey, Nature Physics **13**, 781 (2017).
- ³² K. A. Landsman, C. Figgatt, T. Schuster, N. M. Linke, B. Yoshida, N. Y. Yao, and C. Monroe, Nature **567**, 61 (2019).
- ³³ X. Nie, Z. Zhang, X. Zhao, T. Xin, D. Lu, and J. Li (2019), arXiv:1903.12237v1.
- ³⁴ D. E. Kharzeev and H. J. Warringa, Physical Review D **80**, 034028 (2009).
- ³⁵ N. Armitage, E. Mele, and A. Vishwanath, Reviews of Modern Physics **90**, 015001 (2018).
- ³⁶ A. H. C. Neto, F. Guinea, N. M. R. Peres, K. S. Novoselov, and A. K. Geim, Reviews of Modern Physics **81**, 109 (2009).
- ³⁷ R. Okuyama, W. Izumida, and M. Eto, Journal of Physics: Conference Series **969**, 012137 (2018).
- ³⁸ M. Z. Hasan and C. L. Kane, Reviews of Modern Physics **82**, 3045 (2010).
- ³⁹ C. L. Kane and E. J. Mele, Physical Review Letters **95**, 226801 (2005).
- ⁴⁰ P. Goswami and S. Tewari, Physical Review B **88**, 245107 (2013).
- ⁴¹ A. Turner and A. Vishwanath, *Topological Insulators: Chapter 11. Beyond Band Insulators: Topology of Semimetals and Interacting Phases*, Contemporary Concepts of Condensed Matter Science (Elsevier Science, 2013), ISBN 9780128086926.
- ⁴² A. A. Burkov and L. Balents, Physical Review Letters **107**, 127205 (2011).
- ⁴³ M. J. Klug, M. S. Scheurer, and J. Schmalian, Phys. Rev. B **98**, 045102 (2018).
- ⁴⁴ Y.-G. Chen, X. Luo, F.-Y. Li, B. Chen, and Y. Yu (2019), eprint arXiv:1903.10886.
- ⁴⁵ G. D. Mahan, *Many-Particle Physics* (Springer US, 2000).
- ⁴⁶ G. Giuliani and G. Vignale, *Quantum Theory of the Electron Liquid* (Cambridge University Press, 2005).
- ⁴⁷ J. Rammer and H. Smith, Reviews of Modern Physics **58**, 323 (1986).
- ⁴⁸ D. A. Roberts and D. Stanford, Physical Review Letters **115**, 131603 (2015).
- ⁴⁹ Y. Huang, Y.-L. Zhang, and X. Chen, Annalen der Physik **529**, 1600318 (2016).
- ⁵⁰ X. Chen, T. Zhou, D. A. Huse, and E. Fradkin, Annalen der Physik **529**, 1600332 (2016).